

IMPROVING NANO MATERIAL COATING OF GAS TURBINE BLADES MODEL ANALYSIS

Dr. VODNALA VEDA PRAKASH

*Assistant Professor, Dept. of Mechanical Engineering, KSHATRIYA COLLEGE OF ENGINEERING
KCEA, Armoor.*

Dr. BOMMANA SHRAVN KUMAR

*Assistant Professor., Dept. of Mechanical Engineering, AAR MAHAVEER ENGINEERING
COLLEGE. Hyderabad.*

ABSTRACT

Gas turbine needs to withstand high temperature, stresses and fatigue loads they are exposed to, while still being affordable and maintaining a long-life span. This paper presents an alternative material for Thermal Barrier Coating (TBC) of the gas turbine blade. The paper also summarizes the basic properties of nickel superalloys that are used as a base material for the blades. The simulation study is conducted on the CAD model with and without coating in ANSYS. Most of gas turbine performances evolving coatings on combustion chambers because of its high temperature withstand ability improves combustion process.

As a part of this some works which is considerable for improving performances stage wise compressor blades also coming in to consideration. Deterioration of blades also affects total performance of turbine, this leads to engine performances depended on gas turbine efficiency. In order to stream line minimum gaps occurred in long life cycles of gas turbine linked engines thermal stresses on blades also becoming a needful factor of research.

1. Introduction:

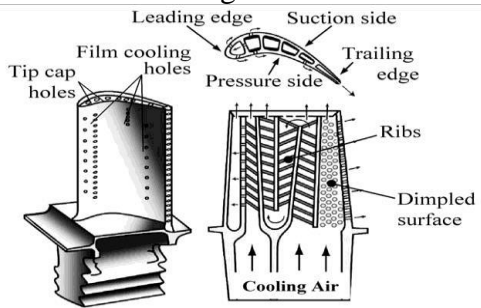
Gas turbines work at very high-temperature ranges of about 1200°-1500°, to withstand

these high temperatures, it is necessary to insulate the components thermally. Thermal barrier coatings are used for this purpose. Thermal Barrier Coatings (TBCs) allow the parent material to operate cooler. They perform the important function of insulating components, such as gas turbine, aero-engine parts, operating at elevated temperatures (e.g. turbine blades, combustor cans, ducting and nozzle guide vanes). TBCs are characterized by very low thermal conductivity. Either of these may be done by adding heat so that the temperature of the working fluid is increased after compression. To get a higher temperature of the working fluid, a combustion chamber is required where combustion of air and fuel takes place giving temperature rise to the working fluid. The turbine escapes energy from the exhaust gas. The analysis of turbine blade mainly consists of the following two parts: Structural and thermal analysis. The analysis is carried out under steady state conditions using ANSYS software. The study has been conducted with two different materials Inconel 718 and Titanium T6.

Turbine Blade Cooling:

Turbine components are placed right after the combustor and are therefore, subject to the highest temperatures in an engine. The turbine blades are directly in the line of fire (so to speak) of these incredibly high temperatures. Higher temperatures yield higher cycle efficiencies,

meaning that the limit on efficiency for a cycle is determined by turbine materials. The current state of the art materials can only give so much heat resistance capacity, which makes blade cooling essential. In this post we'll be taking a look at the various cooling methods that exist for turbine blades, and the tools to design them. The mean rotor blade temperature is about 3500C below the prevailing gas temperature after efficient blade cooling as shown below in figure



Turbine Blade Materials:

Advancements made in the field of materials have contributed in a major way in building gas turbine engines with higher power ratings and efficiency levels. Improvements in design of the gas turbine engines over the years have importantly been due to development of materials with enhanced performance levels. Gas turbines have been widely utilized in aircraft engines as well as for land based applications importantly for power generation. Advancements in gas turbine materials have always played a prime role – higher the capability of the materials to withstand elevated temperature service, more the engine efficiency; materials with high elevated temperature strength to weight ratio help in weight reduction. A wide spectrum of high performance materials - special steels, titanium alloys and super alloys - is used for construction of gas turbines .The material available limits the turbine entry temperature (TET).the properties required are as follows

- (a) tensile strength
- (b) resistance to high frequency vibration fatigue stresses
- (c) low frequency thermal fatigue stresses
- (d) resistance to erosion and corrosion

ANALYSIS RESULTS:

**TABLE 1
Loads**

Object Name	Temperature	Heat Flux	Heat Flow
Magnitude	1200. °C (step applied)	4.63e-006 W/m ² (step applied)	200. W (step applied)

**TABLE 2
Results**

Object Name	Temperature	Total Heat Flux	Directional Heat Flux	Thermal Error
Results				
Minimum	21.302 °C	1.3369e-003 W/m ²	-06 W/m ²	4.3683e-013
Maximum	1201.2 °C	5.0516e+007 W/m ²	1.5858e+007 W/m ²	1.3289e+005

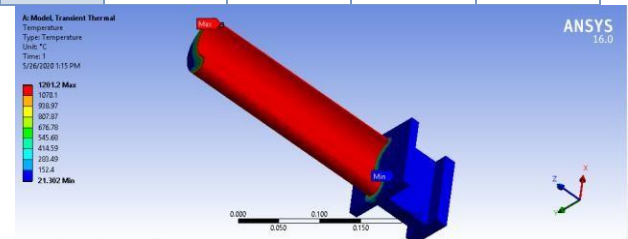


**Figure:
Temperature**

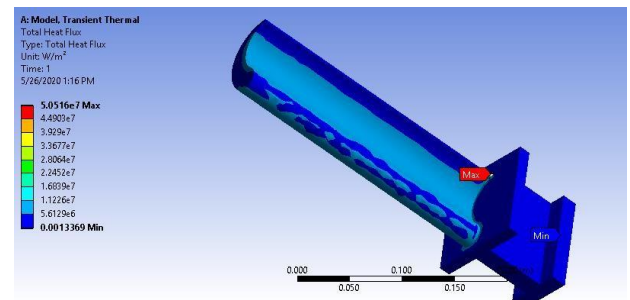
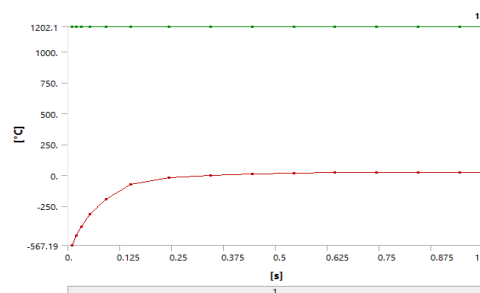


**FIGURE 7
Total Heat Flux**

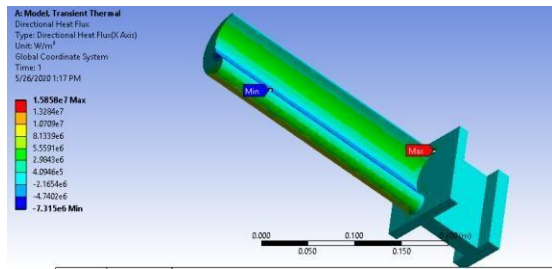
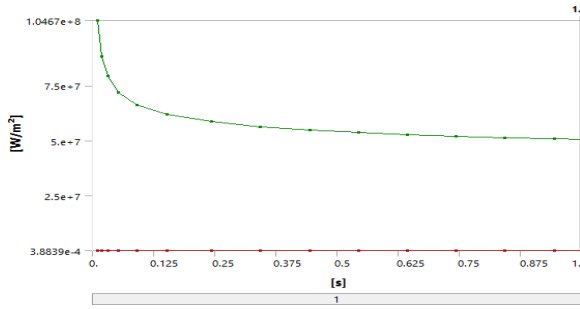


Figure:
Directional Heat Flux

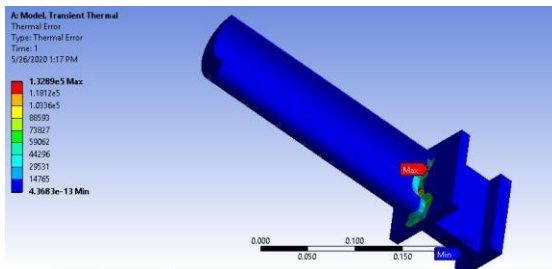
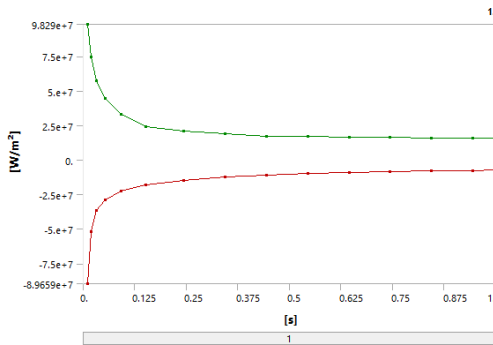
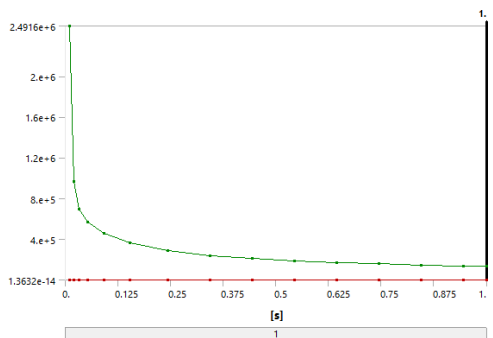


Figure:
Model (A4) > Transient Thermal (A5) > Solution (A6) > Thermal Error



Graph: turbine blade analysis comparison three materials and variations

Full scale Blade LE - Relative flow angle:

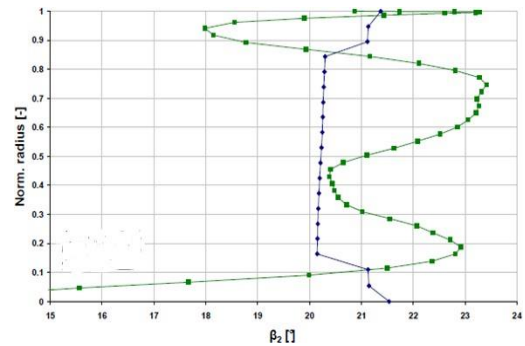


Figure: Inconel material stream edge at cutting edge trailing edge

So as to acquire bay relative stream edges at center point and tip from Multall06 results in Figure line be embedded from an extrapolation among two point at approximately 10 and 90 percent of standardized range. Explanation behind this behavior at limit. At district towards cutting edge center point and tip numerous complex flow design influence edges significantly as can be found in Figure It would have been absurd to configuration precisely to see since don't speak to flow all in all at center and tip.

Full scale cutting edge LE - Relative stream point

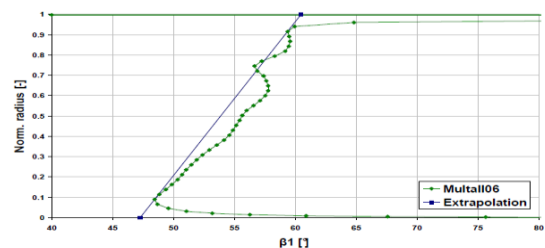


Figure: B6F - Approximation of relative stream edge at driving edge

Outlet relative stream edge changes impressively over cutting edge length. This be an impact of auxiliary stream vortices. Plentifulness of variety however be generally little, only couple of degree, barring qualities close to center. In diagram utilized for deciding

cutting edge channel metal point impact of 2 b be little particularly in area being considered.

Full scale Blade TE - Relative stream point:

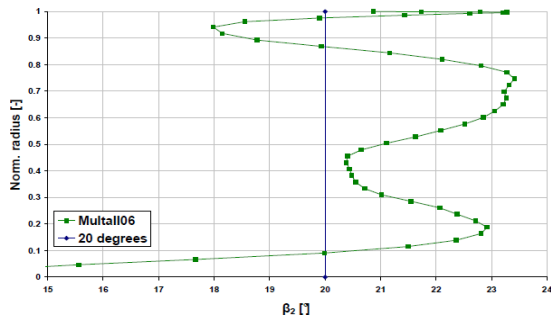


Figure: 4-8 B6F Guess of relative stream edge at sharp edge trailing edge

Stream edges include be gotten just via perusing of x-hub at 0, 50 and 100 percent of standardized span. In table beneath, edges utilized as contribution toward Prof. Mamaev's relationship from data above and ensuing metal plot for B6F have the capacity to seen reliant on both Beta2 furthermore, Multall06 consequences.

Full scale Blade LE – Incidence:

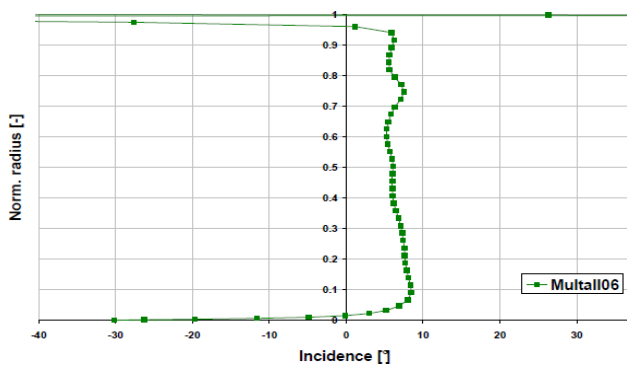


Figure: Full scale Blade LE – Incidence



Figure: Examination at midriff through B6F and reference sharp edge

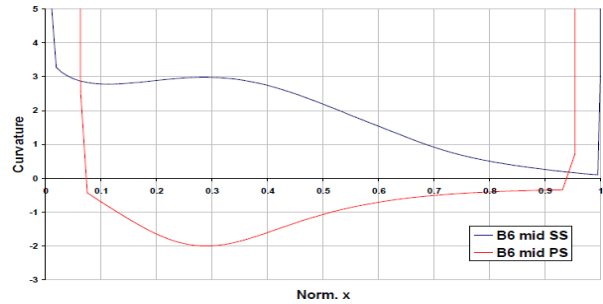


Figure: Bend division at mid area B6

Table 6.16: Curvature division at hub section B6

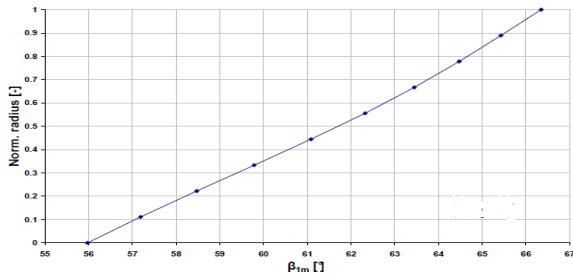
	D	D opt
Tip	0.157	0.21
Mid	0.159	0.22
Hub	0.152	0.23

Design - B6

detail of hot geometry of B6, both in full and model scale be exhibited now and can be seen represented in Table 8. Particularly essential be point of view degree and measure of sharp edges of proposed structure which be lower than common gas turbine respects. purpose for be, as referenced prior, intentional decision in light of conceivable social affair deterrents. This low perspective extent toger through relative low number of sharp edges be quick result of decision to extend center point amicability.

Table: detail of hot geometry of B6

Blade parameter	B6F (FORGED STEEL)	B6M (INCON EL)	4b (EN36)
rhub [mm]	430.44	177.50	177.50
rtip [mm]	493.97	203.70	204.80 (entry)
bhub [mm]	75.65	31.20	26.11
bmids [mm]	76.46	31.53	26.14
btip [mm]	77.46	31.94	26.14
Tip clearance [mm]	0.73	0.30	0.20



Graph: B6 M Metal angle



Figure: 4-22 B6M

Boundary circumstances:

Since aggregate to static weight degree of reference make be to developed, add up to weight was set at strait and static load at outlet. Objective was to compose twisting course of aggregate strain to evaluated information from test turbine as delta condition. In any case, in context of soundness issues in CFX, with pivot at channel, add up to weight was approximated as unflinching over range. This was related as limit condition for all of endeavors with target that outcomes could be looked. impacts on result caused by this guess be recognized to be irrelevant aggregate cove temperature was appeared unsurprising with range exceptional concurrence through ensured profile given via test turbine blower at any rate set estimation of 345 K is genuinely over target propelling power in Table 1.

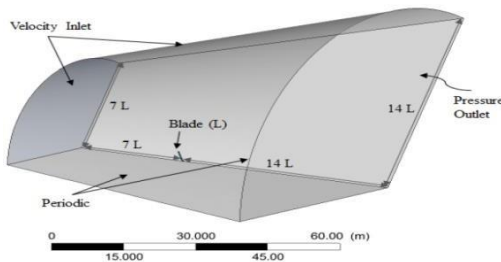
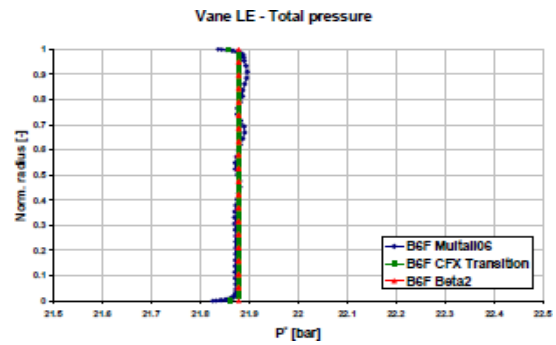
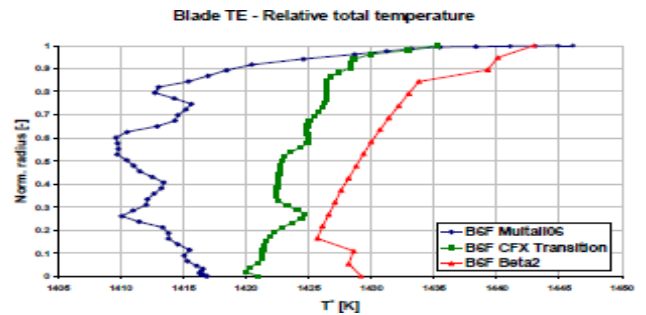


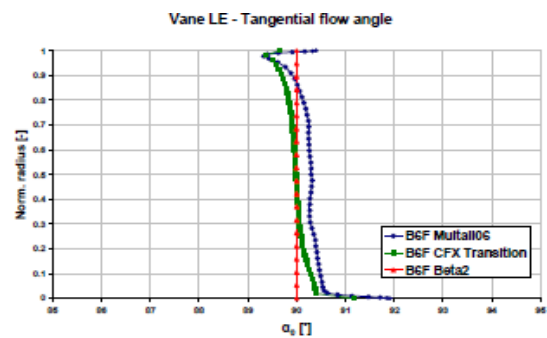
Figure: Domain size and boundary description



Graph: Vane LE – Total pressure of Boundary conditions



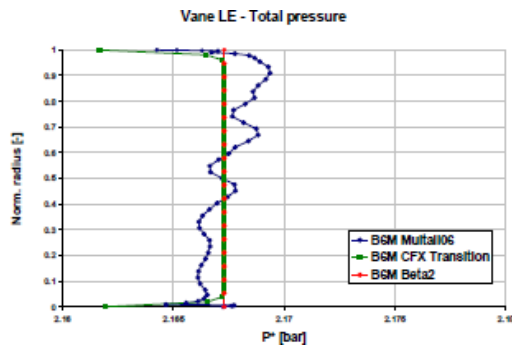
Graph: Blade TE – Relative total pressure of Boundary conditions



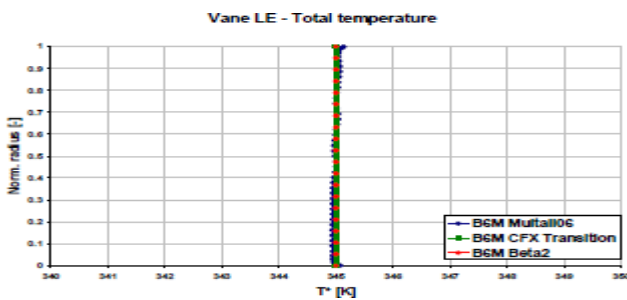
Graph: Vane LE – Tangential flow angle of Boundary conditions

B6M:

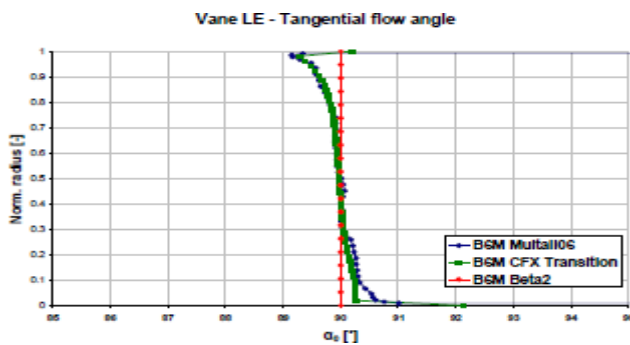
Extended courses show undefined examples from in full scale case. Once more, CFX predicts chop down static burdens and higher Mach numbers next to at edge trailing edge separated through Beta2 and Multall. Understanding among Multall and CFX through regard to digressive stream point sharp edge driving edge be spared to show scale. This shows metal edge be fittingly organized within like manner at model scale.



Graph: Vane LE – Total pressure of B6M



Graph: Blade TE – Relative total pressure of B6M



Graph: Vane LE – Tangential flow angle of B6M

Configuration Point Analysis:

At setup point condition, turbine stream field was settled using CFD approach and each front line push (NGV and rotor) was explored uninhibitedly. stream attributes in central and furthermore basic areas be considered, as close center point and tip zones, and also conventional qualities for a few parameters at stage delta and outlet regions. Static weight transport along every sharp edge profile be plotted against its concordance to overview direct of stream along edge weight and suction

sides. Sharp edge profile be multi-roaming circuitous segment (MCA)

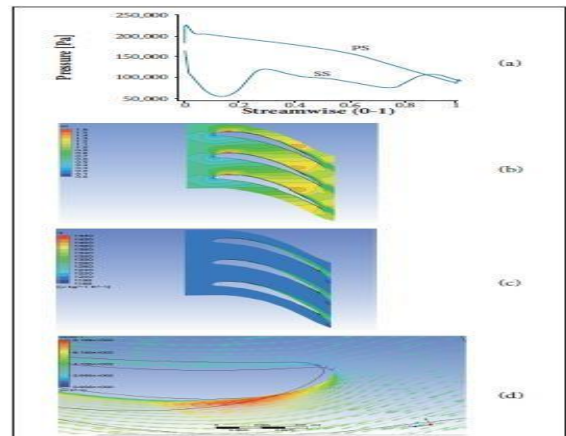


Figure: NGV spanwise - 20% (a) Static weight assortment along bleeding edge agreement; (b) Mach number shapes; (c) Entropy frames; (d) Velocity vector

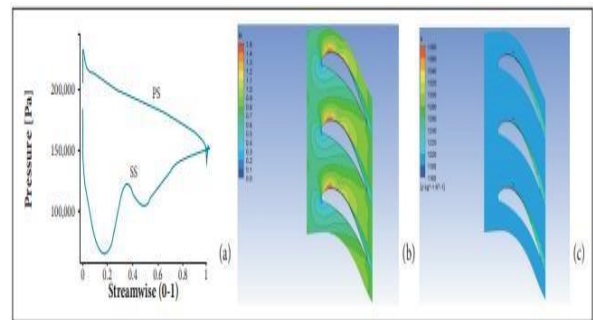


Figure: NGV spanwise - 80% (a) Static weight assortment along edge amicability; (b) Mach number structures; (c) Entropy shapes

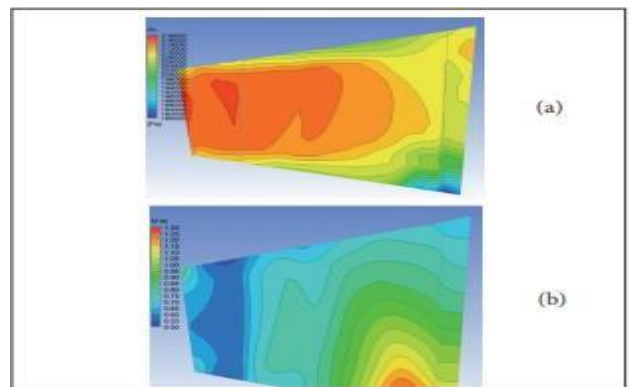


Figure: NGV — edge to-cutting edge mid plane (a) Total weight appropriation forms; (b) Mach digit shape

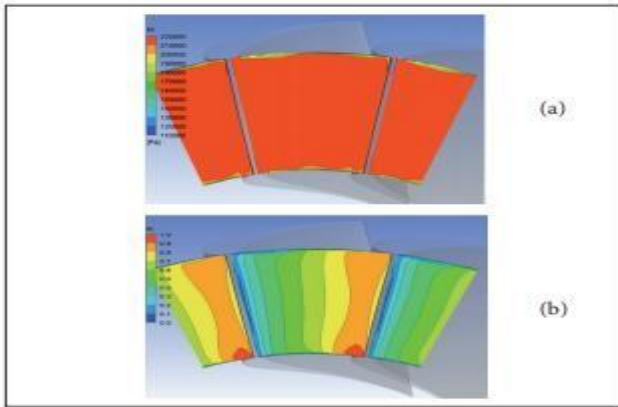


Figure: NGV delta (a) Total weight frames; (b) Mach number shape

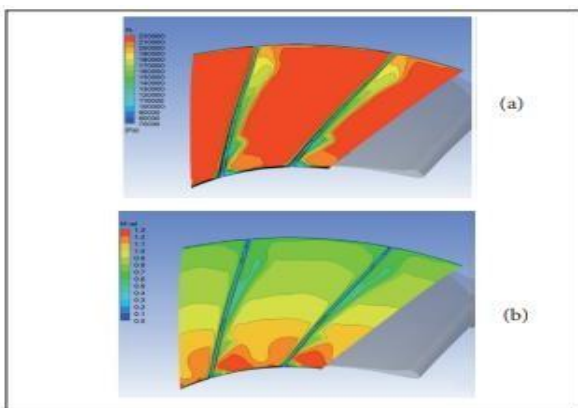


Figure: NGV outlet (a) Total weight frames; (b) Mach number shape

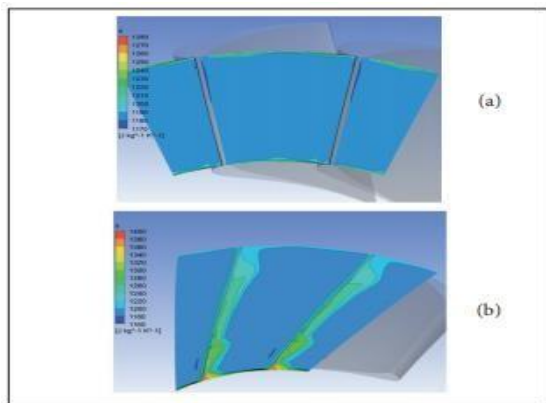


Figure: Entropy shapes (a) Stator channel; (b) Stator cove

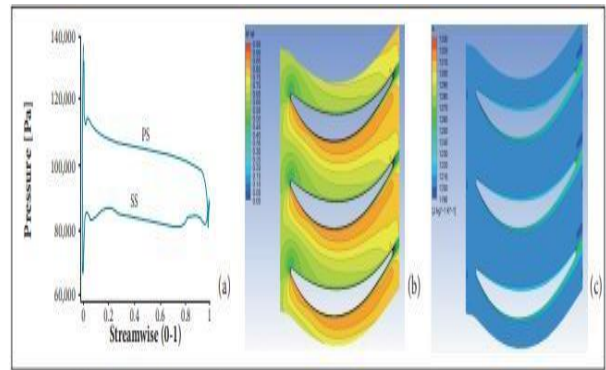


Figure: (a) Static weight assortment at 20% of rotor spanwise (b) Mach number structures at 20% of rotor spanwise (c) Entropy shapes at 20% of rotor front line length

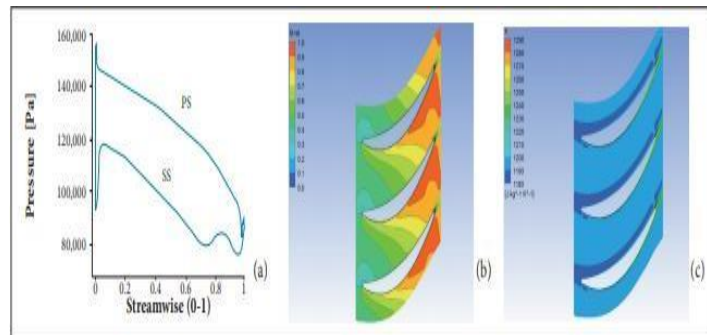


Figure: (a) Static weight assortment at half of rotor spanwise; (b) Mach number shapes at half of rotor spanwise; (c) Entropy frames at half of rotor bleeding edge run

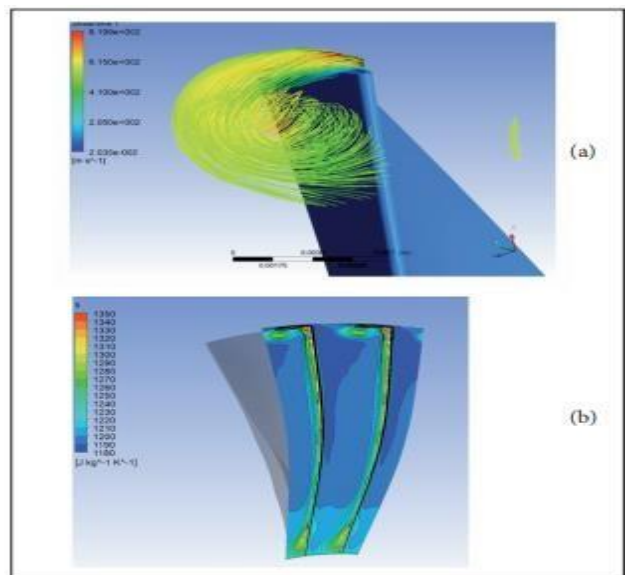


Figure: (a) Streamlines since of rotor tip space; (b) Entropy shapes at rotor outlet

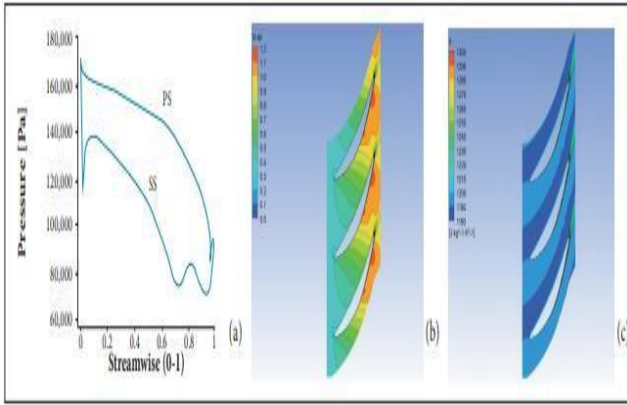


Figure: (a) Static weight assortment at 80% of rotor spanwise; (b) Mach number structures at 80% of rotor spanwise; (c) Entropy shapes at 80% of rotor edge length

In perspective of CFD results, turbine be smother at design point conditions. This be commonplace and be in simultaneousness via turbine structure logic and infers that high essentialness move occurs in gas advancement process. Doubtlessly an arrangement of couple of coefficients used in incident showing should be adjusted to upgrade turbine conjecture for execution calculations.

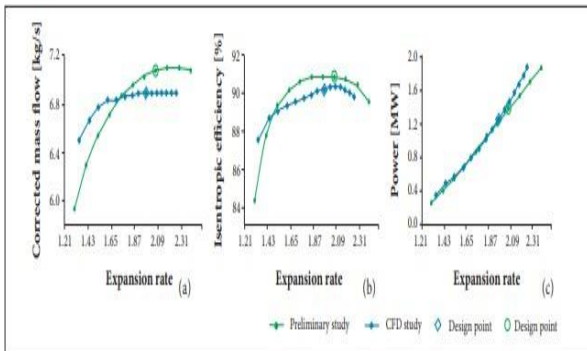
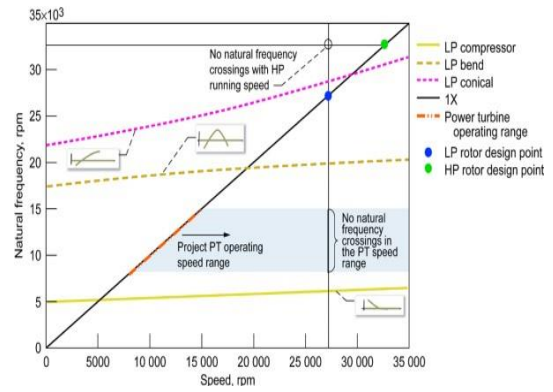
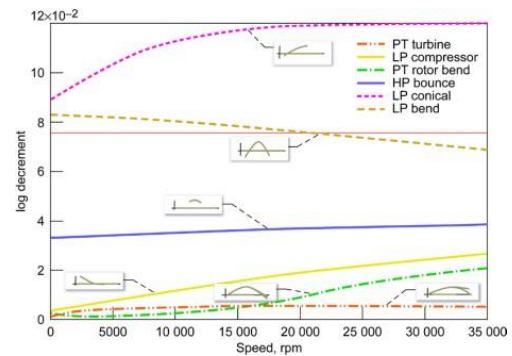


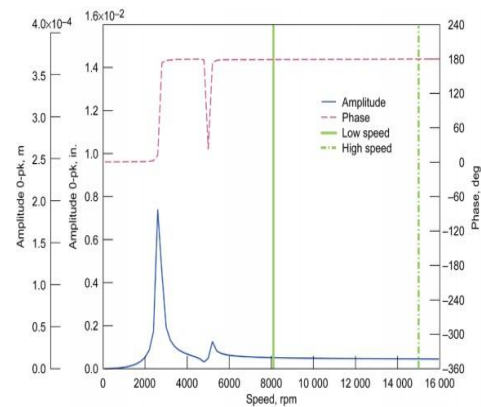
Figure: (a) Redressed mass stream; (b) Isentropic proficiency; (c) Power versus development rate



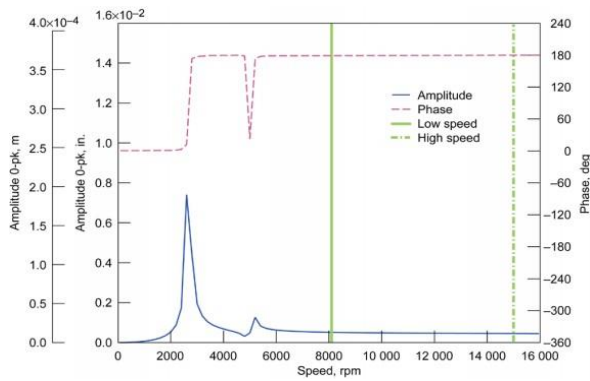
Graph: Diagram Showing LP Natural Frequencies and Projections of PT and HP Excitation Frequencies



Graph: Stability Map for LCTR2 Concept Engine



Graph: Bode Plot for LCTR2 Power Turbine Rotor



Graph: Bode Plot for the LCTR2 Power Turbine Rotor

Table: Efficiencies for minimum and maximum TE radii for rotor phase angle variation cases

Turbine	Particle radial loading % span	Maximum local erosion rate (mg/g/cm ²)	Overall blade erosion rate (mg/g)	
			Stator	Rotor
Coated blades	10%	83.65(Rotor suction side)	0.87	0.96
	100%	34.58(stator suction side)	0.89	0.94
Non-Coated blades	10%	79.56(Rotor suction side)	1.56	0.92
	100%	25.64(stator suction side)	0.93	0.75

Figure: TBC disintegration rates on sharp edge surface for uniform molecule

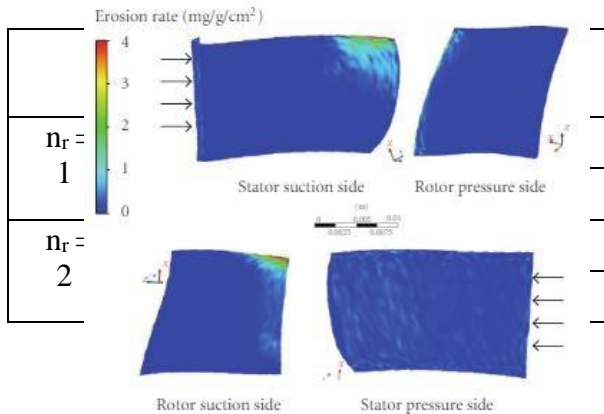
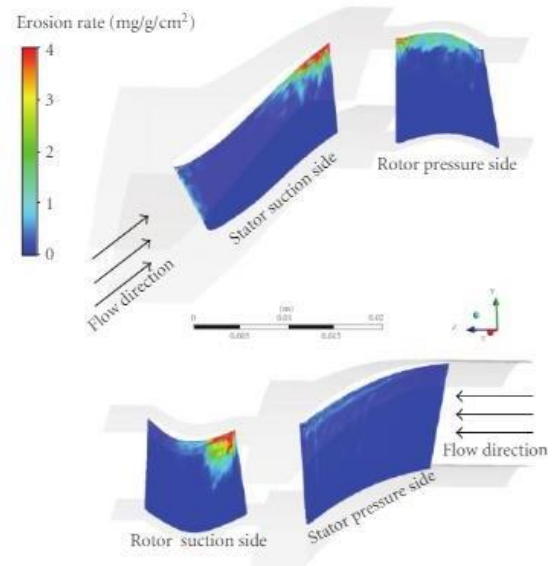


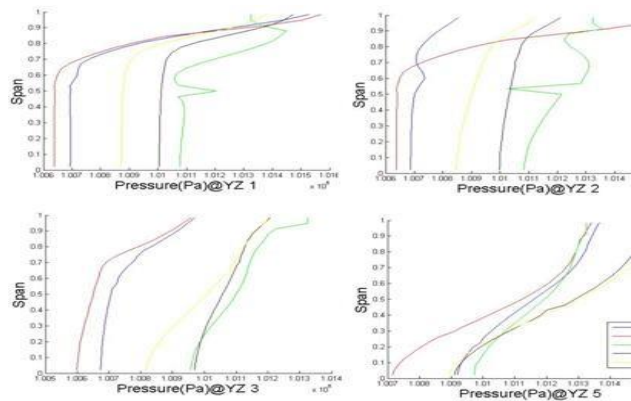
Figure: TBC disintegration rates on cutting edge surface in business turbine for uniform molecule stacking at half of gas speed

Table: TBC disintegration rates on cutting edge surface in business turbine for particle seeding inside 5% of stator edge length close to center point and cover at half of gas speed



stacking at half of gas speed.

TBC disintegration rates on sharp edge surfaces in NASA-structured turbine for particle seeding inside 10% of stator cutting edge range close to center point and cover at half of gas speed.

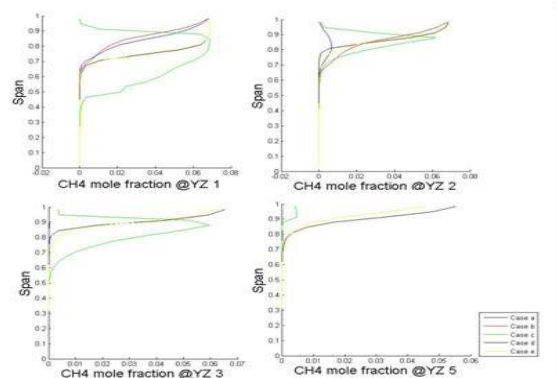


Graph: Pressure (Pa) @ YZ 1,2,3,5

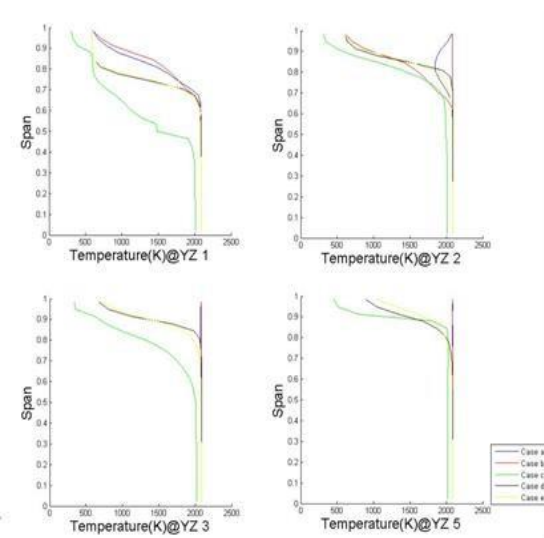
Pressure profile:

It creates impression that case and case b concurs through one anor while case c, d and e concur by means of one anor. Purpose behind this fact be ordinary unevenness models. Two first cases use collections of $k-\epsilon$ while three later cases use $k-\omega$ appear. In light of hypothesis parcel, part 3.5, $k-\omega$ model should demonstrate pervasive estimation of limit layer, along these lines progressively exact calculations of weight

to be evident only 40% of range accomplishes last temperature of 2000K. As stream pushes ahead it will be warmed, In YZ 5 in Figure, around 90% territory accomplishes last temperature, or after stream moves 41% of its way. once more, for cases without warmth trade, after stream moves to YZ 2 or 10% of its way, stream accomplishes its last temperature.



Graph: CH4 mole fraction



Graph: lower temperature due heat transfer

Temperature profile

One can foresee that case c and case e would have chopped down temperature due warmth exchange, and this laid out in Figure 43. In cases c and e, toward start of chamber, YZ 1 in Figure, stream temperature be fundamentally influenced by adjoining temperature, as ought

CONCLUSIONS:

Impact of high temperature presentation on covering execution as far as warm properties was illustrated. Sintering was seen inside microstructure of rmally uncovered examples; prompting significantly expanded warm conductivity. Be that as it may, microstructural changes couldn't be specifically measured with microstructure methods utilized up to this point. While sintering of microstructure affected all coatings; how much warm execution corrupted was dependant on microstructural highlights. Again coatings created with a pore previous showed a littler corruption in execution. Regarding strategies utilized for surveying effect of microstructure (change in structure) and science of coatings; laser

The temperature has a significant effect on the overall stresses in the turbine blades. Maximum temperatures are observed at the blade tip section and minimum temperature variations at the root of the blade. Temperature distribution is almost uniform at the maximum curvature region along blade profile.

Temperature is linearly decreasing from the tip of the blade to the root of the blade section. For all the materials the temperature maximum observed is varying between 7940C to 8120C. Maximum stress induced is within safe limits for all the materials except aluminum. The modal analysis reveals that the fundamental frequency of titanium alloy is highest (35Hz) as compared all other materials. Hence resonance delay for this hence dynamically more stable.

From the Simulation study of the blade model without thermal barrier coating, it is clear that the coating is essential for the gas turbine blade to work efficiently under high temperature. We have carried out an analysis of the blade model with a different coating material. From the static structural analysis, we find that blade coated with Zirconium carbide has lesser induced maximum stress value compared to the other two coating materials. So, it is clear that Zirconium carbide can withstand a higher load compared to the other two materials. From the steady-state thermal analysis, we find that the maximum heat flux value) for the blade model with Zirconium carbide coating is less compared to the other two models. The coating material along with adding strength and thermal resistance to the blade, it should be very light in weight so that the power requirement for the turbine engine should not increase much. So, Zirconium carbide is one of the low-density Ceramic material its best suite alternative for coating of the gas turbine blade.

Future Scope of work:

- To improve the obtained results, further in future; one can increase the coating thickness from 0.5 mm to 1mm or 2 mm by which von-misses stresses and deformation may reduce considerably.
- By providing the holes axially in the blade, may also reduce the temperature of the blade thereby increase the cooling effect which in turn reduces the von-misses stresses and deformation

REFERENCES

1. Abioye, A. A., P. O. Atanda, S. B. Majolagbe, D. A. Isadare, O. P. Abioye, K. J. Akinluwade, A. R. Adetunji (2015), "Material Selection for Gas Turbine Blade Coating Using GRANTA Material Selector", *Advances in Research*, ISSN: 2348-0394, Volume No: 5, Issue No: 1, PP: 1-9
2. Achuta Rao, "Rotor dynamic capabilities in ANSYS Pro-mechanical", ANSYS. 2000
3. Balaji, K., C. Azhagesan, R Vinoth Pandian, N Muthu Murugan, N Aravinth (2016), "Review of Cooling Effect on Gas Turbine Blade", *International Conference on Systems, Science, Control, Communication, Engineering and Technology*, ISSN: 2320-2092, Volume No: 5, Issue No: 4, PP: 478-492
4. Banpurkar, R.D., P.K.Katara (2015), "Review Paper On Stress Distribution Over Blade Of Compressor Of Micro Turbine", *International Journal of Advanced Engineering and Global Technology*, ISSN: 2309-4893, Volume No: 3, Issue No: 7, PP: 870-873
5. Christoph Leyens (2004), "Advanced Materials And Coatings For Future Gas Turbine Applications", *24th International Congress Of Aeronautical Sciences*, ISBN 0-9533991-6-8, Volume No: 7, Issue No: 3, PP: 1-8
6. Christopher Chahine, Tom Verstraete, Li He (2015), "Multidisciplinary Design Optimization of an Aero-Engine Fan Blade with Consideration of Bypass and Core Performance", *11th World Congress on Structural and Multidisciplinary Optimization*, ISSN: 1615-147X, Volume No: 3, Issue No: 2, PP: 1-6
7. Clarkeand, D.R., Levi, C.G (2003), "Materials Design for Next Generation rmal Barrier Coatings", *Annual Review of Materials Research*, ISSN: 1531-7331, Volume No: 33, Issue No: 1, PP: 383-417

8. Girish Modgil, William A. Crossley, Dongbin Xiu (2013), “Design Optimization of a High-Pressure Turbine Blade using Generalized Polynomial Chaos (gPC)”, 10th World Congress on Structural and Multidisciplinary Optimization, Volume No: 5, Issue No: 4, PP: 1-16
9. Gopinath Chintalaa, Prasad Gudimetla (2014), “Optimum material evaluation for gas turbine blade using Reverse Engineering (RE) and FEA”, Procedia Engineering, ISSN: 1877-7058, Volume No: 97, Issue No: 2, PP: 1332–1340
10. Goward, G.W (1998), “Progress in coatings for gas turbine airfoils”, Surface and Coatings Technology, ISSN: 0257-8972, Volumes No: 108–109, Issue No: 2, PP: 73-79
11. Josin George, Titus. R (2014), “ Design and Analysis of First Stage Gas Turbine Blade with a Modification on Cooling Passages Using ANSYS”, International Journal of Latest Trends in Engineering and Technology, ISSN: 2278-621X, Volume No: 3, Issue No: 4, PP: 313-326
12. Julian D. Osorio, Alejandro Toro, Juan P. Hernández-Ortiz (2012), “ermal Barrier Coatings for Gas Turbine Applications: Failure Mechanisms and Key Microstructural Features”, Dyna, ISSN: 0012-7353, Volume No: 79, Issue No: 176, PP: 149-158.